The fabrication of carbon nanotube probes utilizing ultra-high vacuum transmission electron microscopy

2009 Nanotechnology 20 285307

(http://iopscience.iop.org/0957-4484/20/28/285307)

Nanotechnology **20** (2009) 285307 (9pp) doi:10.1088/0957-4484/20/28/285307

The fabrication of carbon nanotube probes utilizing ultra-high vacuum transmission electron microscopy

Shu-Cheng Chin[1], **Yuan-Chih Chang**[1] **and Chia-Seng Chang**

Institute of Physics, Academia Sinica, Nankang, Taipei 115-29, Taiwan

E-mail: jasonc@phys.sinica.edu.tw (C-S Chang)

Received 24 February 2009, in final form 20 May 2009
Published 23 June 2009
Online at stacks.iop.org/Nano/20/285307

Abstract

An application of ultra-high vacuum transmission electron microscopy (UHV TEM) is demonstrated for the fabrication of carbon nanotube (CNT) probes. In this study, all the fabrication processes—such as CNT attachment, CNT orientation manipulation, and apex trimming—are integrated into a single UHV TEM system. The *in situ* work under UHV conditions ($<5 \times 10^{-10}$ mbar) allows us to clean the tip surface at the start of the fabrication process to ensure a good contact between the tip and CNT. Furthermore, the CNT size can be user-selected to meet the various needs for scanning probe microscopy (SPM). Most importantly, the *in situ* trimming enables a multi-walled CNT to have the sharpness of a single-walled CNT. The three advantages mentioned above are designed to improve conventional methods and will be shown in detail as the procedures of CNT probe fabrication by a series of high-resolution TEM images. Finally, we compare the scanned image via our CNT probes and conventional probes, where the typical artefacts coming from the conventional ones are addressed. We believe the technique we have developed here will further enhance the resolution of SPM measurements.

M This article features online multimedia enhancements

1. Introduction

Since Binnig *et al* invented atomic force microscopy (AFM) in 1986 [1], AFM has been widely used to profile the surface topography of semiconductors, metals, organic materials [2], bio-materials [3, 4], etc. These include insulators, of which the surface topography could not be probed via scanning tunnelling microscopy (STM) [5]. For contact-mode AFM, strong tip distortion often occurred because the cantilever operates within the range of the van der Waals force, consequently limiting the resolution of AFM measurements. To overcome this limit, Digital Instruments developed the tapping-mode (TM) AFM using an oscillating cantilever to minimize the tip–surface interaction time [6]. However, geometrical restrictions arising from both the sample surface topography and the pyramidal shape of commercial tips often cast shadows on vertical surface structures, resulting in the urgent need for high-aspect-ratio tips. In contrast, carbon nanotubes (CNTs), first discovered by Iijima in 1991 [7, 8], seemed to be a suitable candidate for the same purpose because of their rigid structure and their small diameters (around 5–20 nm). Soon after their invention, CNTs were applied in 1996 to scanning probe microscopy (SPM) by Smalley's group through their attachment to commercial cantilevers [9]. These CNT probes successfully mapped out deep rectangular trenches via AFM measurements and obtained atomic images via STM measurements [9].

The application of CNT-probed SPM has been widely employed in the recent decades [10, 11]. So far, the conventional fabrication of CNT probes, also known as CNT attachments, has become a repetitive process relying on large quantities of retrievals. In the early development, the attachment of a CNT was performed under an optical microscope (OM) and the performance was checked later with a scanning electron microscope (SEM). More recently, an SEM equipped with precise manoeuvring tools is employed

[1] The two authors, S C Chin and Y C Chang, contribute equally to this paper.

to carry out the process, thus simultaneously making the attachment and examination [12]. Nevertheless, the limited resolution of the SEM usually requires the CNT length to be longer than 100 nm [13]. Such a long length makes the CNT probe prone to bending, as opposed to the rigid commercial AFM tips, resulting in detrimental artefacts on the topography mapping. In addition, the poor vacuum inside the SEM ($\sim 10^{-6}$ mbar) often contaminates the CNT–tip contact under an energetic e-beam illumination. To solve the problem of image resolution, transmission electron microscopy (TEM) is a suitable candidate; however, the synchronization of attachment and imaging must again be compromised. We must additionally cut the commercial cantilever chip to fit a conventional TEM sample holder. Recently, the concept of SPM@TEM, which was developed by Nanofactory Instruments and refers to a combination of an SPM scanner head and a TEM sample holder, has solved the asynchronous problem [14–16]. However, the commercial holders of Nanofactory Instruments are only designed for normal vacuums (normally $\sim 10^{-7}$ mbar in conventional TEM chambers); thus, the vacuum problem of CNT probe fabrication persists. Moreover, it is very difficult to employ transfer within the Nanofactory holder, particularly as the SPM tip and the sample stage are combined in millimetre dimensions. Hence, a design regarding division between the tip holder and the sample holder inside a TEM chamber is absolutely necessary. To date, Takayanagi's group is the only one to have a homemade SPM@TEM setup with divided tip and sample holders designed for UHV TEM system [17]. A UHV SPM@TEM system employing CNT probe fabrication has yet to be developed.

2. Experimental setup: UHV SPM@TEM system

In this paper, we develop a technique which addresses the disadvantages of the conventional methods of CNT probe fabrication mentioned in section 1 by utilizing ultra-high vacuum transmission electron microscopy (UHV TEM). The vacuum is about 5×10^{-10} mbar inside the UHV TEM chamber, which solves the universal vacuum problem of all the conventional methods. Furthermore, all the fabrication procedures are integrated into a single UHV TEM system and can be *in situ* imaged; thus, the success rate will be greatly increased. We will systematically illustrate how we fabricate a CNT probe with a series of TEM images in the following sections.

All the *in situ* work was carried out with a commercial ultra-high vacuum transmission electron microscope, JOEL JEM-2000V UHV TEM, with an accelerating voltage of 200 kV and an e-beam source of LaB_6. The typical vacuum attained by JOEL is about 7.5×10^{-10} mbar for the UHV condition. We can now pump the chamber down to $<5 \times 10^{-10}$ mbar. There are two three-dimensionally (3D) movable holders inside the UHV chamber. The coarse 3D movement is achieved with three commercial one-dimensional steppers, two ANPxy50s and one ANPz100 produced by ATTOCUBE Systems, with a minimum step displacement of 5 nm observed in the TEM. Due to the overshooting problem ($\sim$10 nm) associated with the ATTOCUBE steppers, the fine 3D movement is done with an EBL #4 piezotube (normally used as an STM scanner), divided into four gold-coated electrodes at the outer tube shell and a whole inner gold-coated electrode. By control of the applied biases at the five electrodes, the piezotube is able to have 3D movement on the sub-nanometre scale, which allows the delicate manipulation within every CNT fabrication procedure shown in the following sections. Both the holders are designed to fit the size of commercial AFM cantilever chips. Initially, the synthesized CNTs are fixed onto a gold blade, the size of which also corresponds to that of commercial AFM cantilever chips. When the CNT selection in the first procedure (described in section 3) is finished, we transfer the AFM cantilever into the UHV chamber and exchange the gold blade via two load locks, one to take out the gold blade and the other to transfer the cantilever.

3. Choosing a user-selected carbon nanotube

In the UHV chamber, chemically synthesized CNTs are fixed on a 3D movable stage while the other 3D movable stage carries an electrolytically etched gold STM tip. Both stages are electrode-connected and are initially grounded. The first procedure of CNT probe fabrication is to choose a suitable CNT, i.e., a suitable length and diameter. Figure 1(a) shows the synthesized CNTs, with many values of length and diameter. As figure 1(b) shows, we can choose any CNT size we want by approaching the gold STM tip to a chosen CNT. Then, we attach the CNT onto the gold tip through electrostatic induction by applying a bias to the gold tip, usually about 1 V. Then, a measured current of 4–6 μA or so confirms the successful attachment. (We will show how to enhance the CNT–tip attachment by the e-beam welding method described in figure 5(a).) After the CNT is attached, we increase the bias to 4 V, at which a current of over 100 μA will flow throughout the connected CNT, and the connected CNT will burn off layer by layer to cut off at roughly the central position (figure 1(c)) [18]. The CNT burning mechanism will be interpreted in section 5. By the procedure shown in figure 1, the CNT size can be completely user-selected since the large quantity of the synthesized CNTs is potentially contains all sizes. The high resolution and the *in situ* imaging of UHV TEM of this procedure solve the problems entailed by the conventional methods, the poor resolution of which rendered us unable to select the CNT size with OM and limited the SEM-selected CNT length to at least 100 nm.

4. *In situ* removal of contaminants

In the second procedure, we have to put the AFM cantilever into the chamber by replacing the synthesized bundle CNTs on their 3D movable stage. In fact, the gold STM tip and the TEM system form a similar mechanism to the STM@TEM mentioned in section 1, which means that a TEM imaging system is equipped with a STM scanner. However, there have been few examples of STM@TEM designed for UHV system and the holder is only longitudinally movable in one

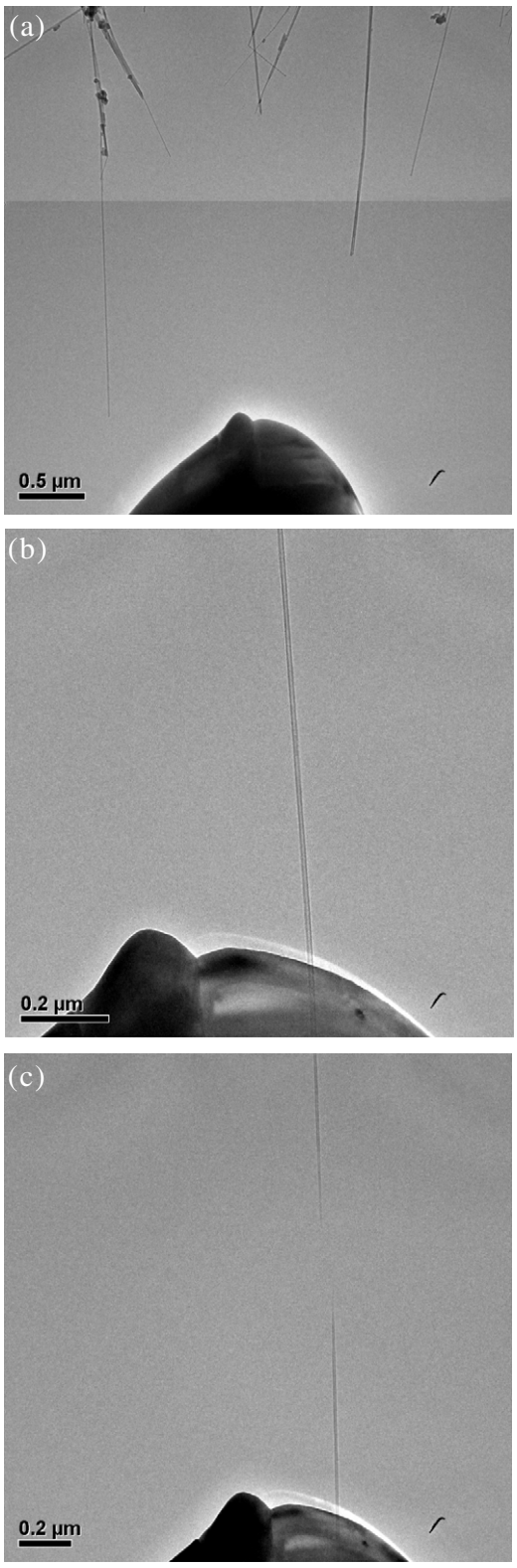

Figure 1. The TEM images show how we choose a CNT with the size we want. (a) There are many sizes of CNT and we approach the gold STM tip to the selected CNT. (b) We apply a bias at 1 V or so to the gold tip, resulting in the selected CNT being attached onto the gold tip via electrostatic induction. The attached portion can be observed with the shadow behind the gold tip. (c) A current of approximately 100 μA will flow through the attached CNT when we increase the bias to 4 V and the CNT will burn off layer by layer to cut off at roughly the central CNT position.

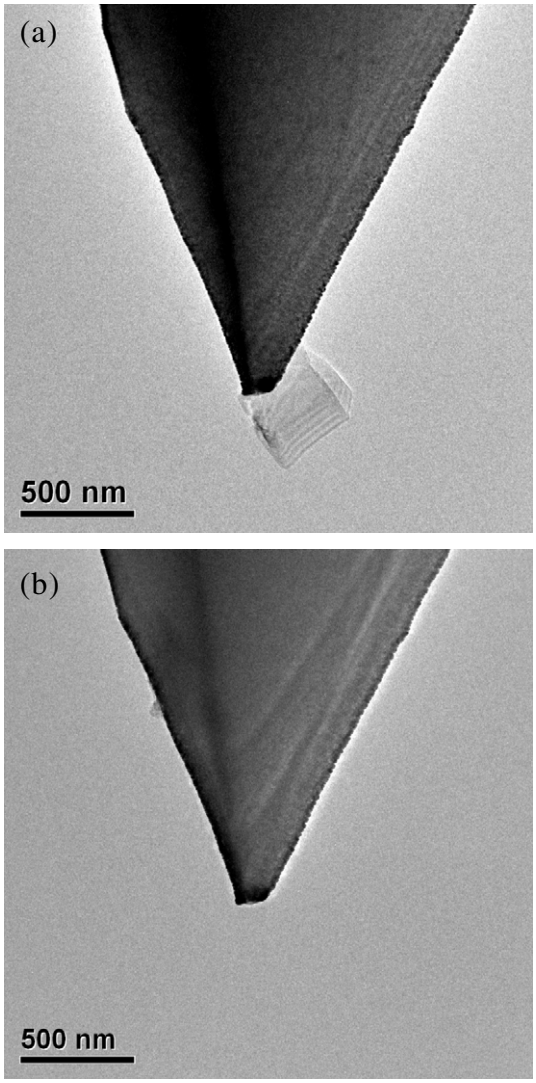

Figure 2. The TEM image in (a) shows how we take off the contaminant on a new cantilever tip via the CNT finger in figure 1(c), which leads to a clean cantilever tip in (b).

dimension [16, 19]. The advantage of our system is that the entire STM@TEM system formed by two 3D movable holders is inside the same UHV chamber. Furthermore, we have designed the holder for the AFM cantilever ourselves, which means that we do not have to cut the cantilever chip to fit a conventional TEM holder. Furthermore, the AFM@TEM and STM@TEM can be user-selected. Figure 2(a) shows an unused cantilever with a contaminant on its tip. Commercial cantilevers are normally preserved in air with only simple humidity control, often causing suspended substances to be adsorbed on the cantilever. Using the conventional SEM method of CNT attachment, we have no method of addressing this problem; thus, the only solution is to throw away any new cantilever with a contaminant. Therefore, the conventional OM method undoubtedly fails. However, we can take away the contaminant via a nano-finger inside the chamber, a concept first suggested by Binnig and Rohrer in 1999 [20]. In figure 1(c), the left CNT attached on the gold tip not only functions as a CNT that is intended to be an SPM probe but

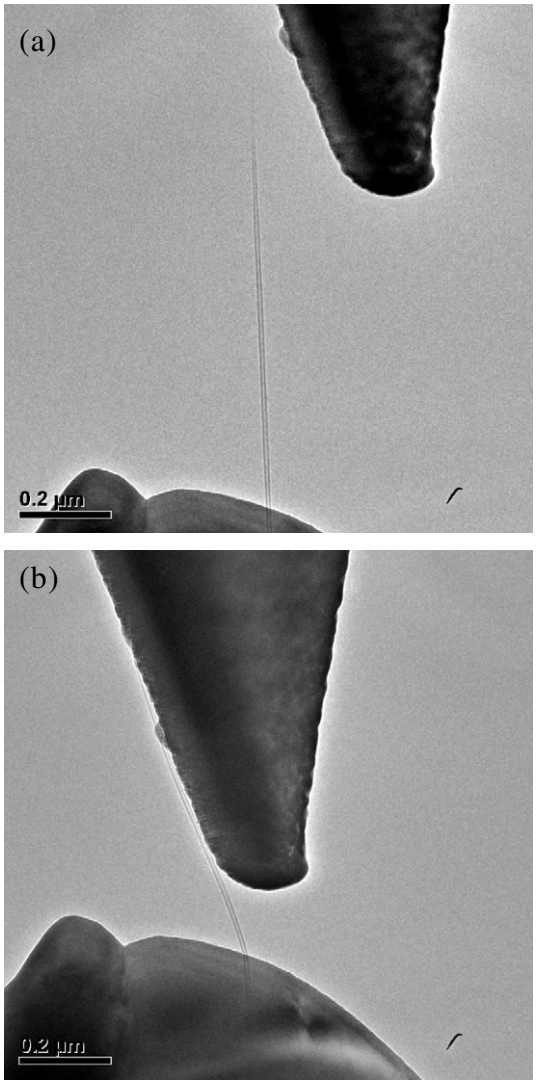

Figure 3. (a) The TEM image shows the approach of the CNT to the cantilever tip. (b) We let a large portion of CNT be attached onto the metal-coated tip surface to make a strong attachment. Thus, the CNT can avoid falling off during strong force measurement.

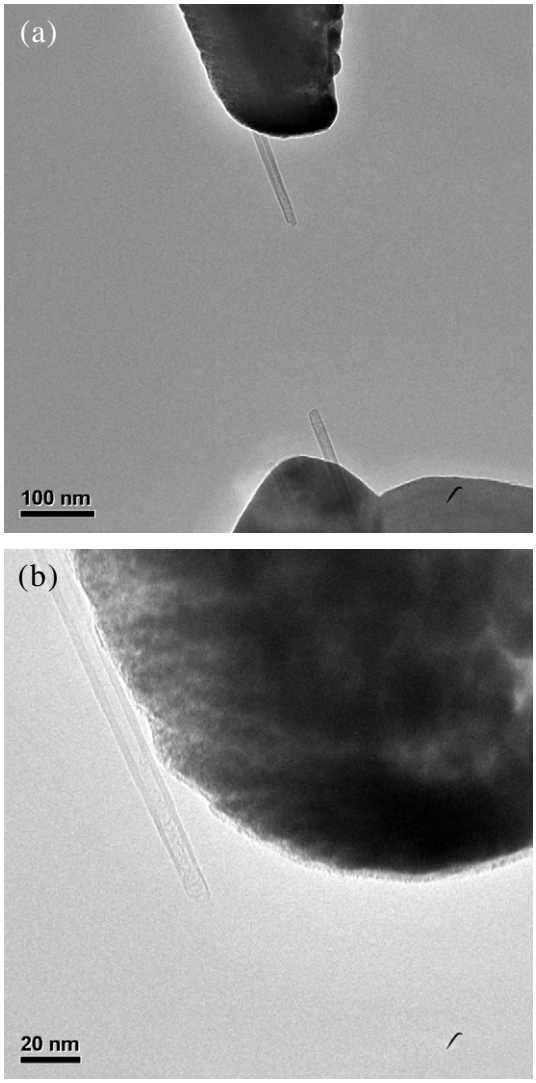

Figure 4. Two TEM images show the influence of the CNT bending on the burned point. (a) The CNT bending is minimized so that we can produce a typical CNT probe. (b) The bending results in a locally higher resistance. The CNT burns at the bending point.

also acts as a finger inside the UHV TEM chamber. We can move the CNT finger to touch the contaminant and force it to drop, as the clean tip displayed in figure 2(b) shows.

5. Fabrication of carbon nanotube probes

To attach the CNT onto the cantilever tip, the cantilever is usually metal-coated with materials such as gold, chromium, platinum, titanium, etc (figure 3(a)). As shown in figure 3(b), we let a large portion of the CNT contact the tip surface. By applying a bias either at the gold STM tip or at the cantilever, the CNT will be again attached onto the metal-coated tip surface via electrostatic induction (the same mechanism as that in figure 1). The large contact surface area results in a strong attachment between the CNT and the cantilever tip and prevents the CNT from falling off during the whole process. Ideally, when a large enough current flows through the CNT, the CNT will burn off layer by layer at its central part (figure 4(a)) [18]. This burning mechanism is interpreted in the following scenario. When an electron current flows through the CNT (without any bending), the heat will initially be uniformly generated along the CNT. However, the two ends are connected to rather bulky metal electrodes, where the heat can be quickly conducted away via the metal contacts. Thus, the temperatures near the two ends are usually lower than the central portion. Consequently, the CNT will cut off due to heat accumulation at the approximate geometrical centre of the CNT.

We can easily control the effective length of a CNT probe by controlling the non-contact CNT portion in figure 3(b). This control allows us to produce a CNT probe less than 100 nm in length, something that the conventional method was not able to do. Due to the limited resolution of SEM, SEM cannot image CNTs shorter than 100 nm, so a conventional CNT probe is normally about 200 nm or longer [8, 21]. The excessive length of the CNT probe leads to a flexible CNT structure, which lowers the precision of topography measurement. (The AFM

images taken with an excessively long CNT probe will be discussed in section 7.) Combining the high resolution of TEM and the *in situ* attachment of our system solves the problem of overly long CNTs. In this procedure, we must take note of the CNT bending at the points of connection in figure 3(b). If the bending is minimized, the non-contact portion will cut off as figure 4(a) appears. If the bending is greater, the consequential lattice distortion will induce additional local strain at the bending point, at which the local periodic potential of the helical graphite lattice changes, in turn raising the local electron scattering rate. From a macroscopic view, the resistance of the bending point will increase and produce more heat when a current flows through the CNT. Thus, the CNT will cut off at the bending point instead of at the geometrically central portion, as on a non-contact CNT (figure 4(b)), and the CNT in figure 4(b) is hard to use because of its very short exposed segment. For the bending condition in figure 3(b), it is sufficient to produce a typical CNT probe as that in figure 4(a). In figure 4(a), there is the problem of CNT orientation tilt. The conventional solution was to employ the CNT probe to scan a grating for hours, causing the CNT orientation to become perpendicular to the scanned surface (usually about 15° tilt to the pyramid tip) [22]. In figure 4(a), we can observe another segment of CNT left on the gold STM tip. From the 3D sub-nanometre positioning capability of our holders mentioned in section 2, the remnant CNT can be regarded as a nano-finger to touch the overly tilted CNT probe again and easily adjust its orientation. This procedure is similar to that for the *in situ* removal of contaminants in section 4. However, tuning the orientation is much more difficult than removing contaminants because the CNT's dimension (∼10 nm) is much smaller than the contaminants (∼1 μm). Therefore, we have to use the remnant CNT on the gold STM tip, which has the same dimension as the CNT probe, and engage the STM piezotube function to achieve the tuning work with sub-nanometre precision. As a result, the method of tuning the CNT probe via a nano-finger merely takes a few minutes, as opposed to the time-consuming conventional method. We have displayed the orientation adjustment process in video 1 (available at stacks.iop.org/Nano/20/285307).

After successfully producing a CNT probe, we zoom in on the region of the CNT–tip interface to the highest possible magnification in figure 3(b). This procedure is used to focus the high-energy electron beam for welding the CNT onto the tip. It makes the CNT attachment stronger and is important for conductive SPM measurements because the bias is ensured to be applied to the CNT tip [23–25]. Figure 5(a) displays an adequate contact between the CNT and the tip. Although this procedure can be done in SEM [26], the poor vacuum (∼10^{-6} mbar) inside the SEM always contaminates the whole cantilever, especially when additional heat is generated from exposure to a focused e-beam. In figure 5(b), we can see an amorphous layer covering the surface of a CNT probe after suffering an e-beam exposure inside the SEM. However, the ultra-high vacuum (<5 × 10^{-10} mbar) of our system prevents the contamination. We have further found that the amorphous layer also disappears after e-beam exposure inside the ultra-high vacuum transmission electron microscope (UHV TEM)

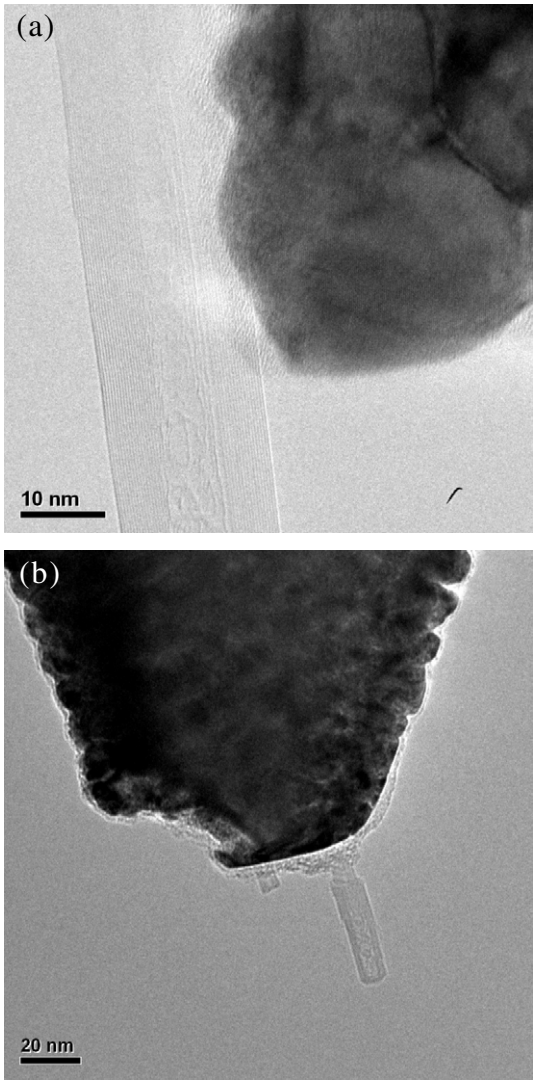

Figure 5. (a) The HRTEM image shows that the CNT is tightly welded onto the metal-coated tip surface via e-beam (200 keV) exposure inside the UHV TEM chamber. (b) However, the e-beam (normally 5–15 keV) inside a conventional SEM contaminates the CNT probe with an amorphous coating layer.

for several minutes. The amorphous coverage due to storage in air is intrinsic and always plays a detrimental role in the fabrication of CNT probes. Our UHV TEM technique has eliminated this detrimental influence.

6. Trimming the apex of carbon nanotube

We have mentioned that the CNT will burn off layer by layer when a current flows through it [18]. Due to this phenomenon, the cut-off point, or the apex, of the CNT probe will go into the shape of a telescope if we carefully adjust the current, as shown in the high-resolution TEM (HRTEM) image in figure 6. Hence, careful adjustment of the current is utilized to trim the apex. As we can see in figure 6, the apex is approximately less than 5 nm-sharp, as sharp as a single-walled carbon nanotube (SWCNT). Theoretically, the sharpness of a SWCNT probe is absolutely unique [27, 28]. Nevertheless, the relatively more

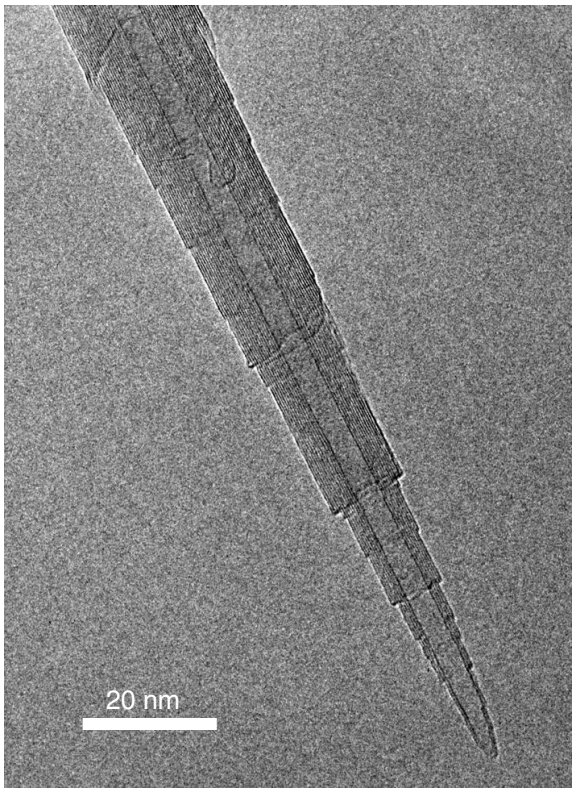

Figure 6. The HRTEM image shows we can *in situ* trim the apex to less than 5 nm, as sharp as an SWCNT. The MWCNT is used for the tip base to prevent flexibility.

flexible SWCNT restricts the measurement resolution more than the multi-walled carbon nanotube (MWCNT) has. The artefact induced by the relatively soft CNT will be discussed later. We again ameliorate the problem of flexibility using *in situ* trimming inside the UHV chamber. The CNT probe in figure 6 has a sharp apex like a SWCNT and a MWCNT as its base to enhance the probe rigidity [29, 30].

7. Carbon nanotube probed AFM measurement

A CNT probe was produced using the aforementioned procedures by our UHV TEM system, as shown in figure 7(a). Except for some impurities at the higher region, we can observe no contaminant near the CNT that could cause perturbations during scanning. The CNT is less than 100 nm in length, minimizing the flexibility effect. Furthermore, the apex is trimmed to less than 5 nm, and its sharpness seems capable of resolving minute characteristics during topography measurements. We have done a simple test on our CNT probe quality in the UHV chamber, which is recorded in video 2 (available at stacks.iop.org/Nano/20/285307). Figure 8 is comprised of six typical tapping-mode (TM) AFM images showing the topography of a GaN thin film; figure 8(a) is scanned by a conventional AFM probe, while figure 8(b) displays the fine surface structure of the same sample obtained via the CNT probe of figure 7(a). That the lateral resolution is <5 nm is confirmed by the various sizes of the grains in figure 8(b). On the other hand, figures 8(c)–(f) are the images

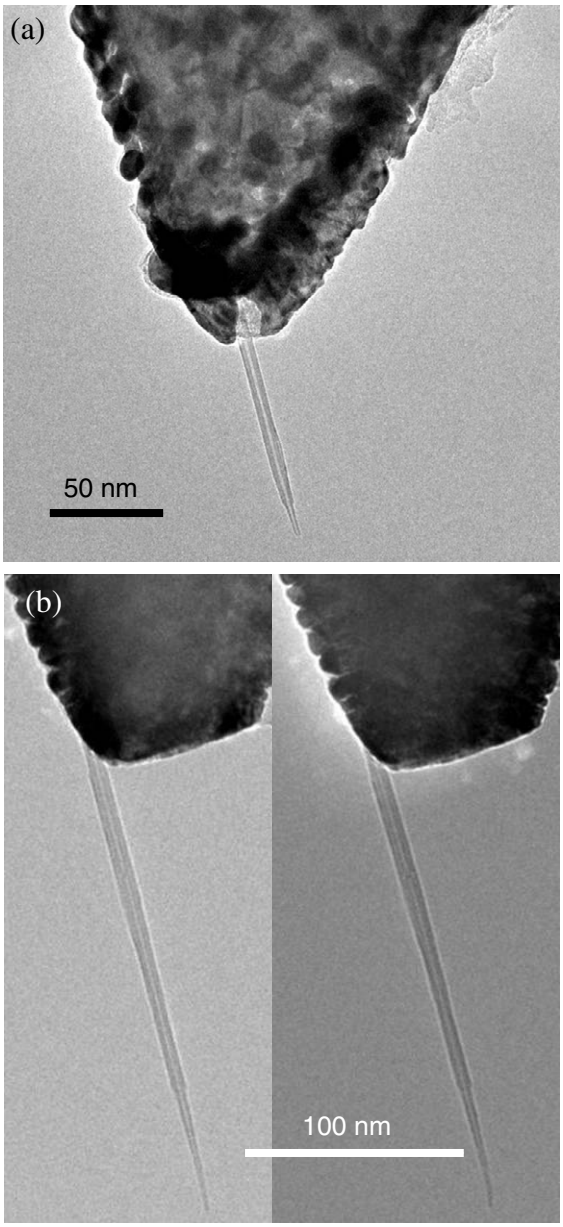

Figure 7. (a) The CNT probe, fabricated by our UHV TEM, less than 100 nm in length and 5 nm in sharpness, is suitable for topography measurement. (b) A CNT probe of around 200 nm in length was specifically made by the conventional method in order to compare the topography measurements between these two probes. The two images display the same CNT probe before (left side) and after (right side) AFM scans.

of the topography obtained by a relatively long and flexible CNT produced by the conventional method [22], which is shown in figure 7(b). Apparently, both the CNT probes can reach a better resolution (referring to figures 8(a)–(c)) but, compared with figure 8(b), figure 8(c) appears slightly inferior in its image resolution. The reason may be attributed to the flexibility of the long CNT that usually lowers the precision of topography measurements.

Figures 8(d) and (e) display two kinds of artefacts induced by the conventional CNT probe. Sometimes, figure 8(b) would appear as figure 8(d), showing many concaves at

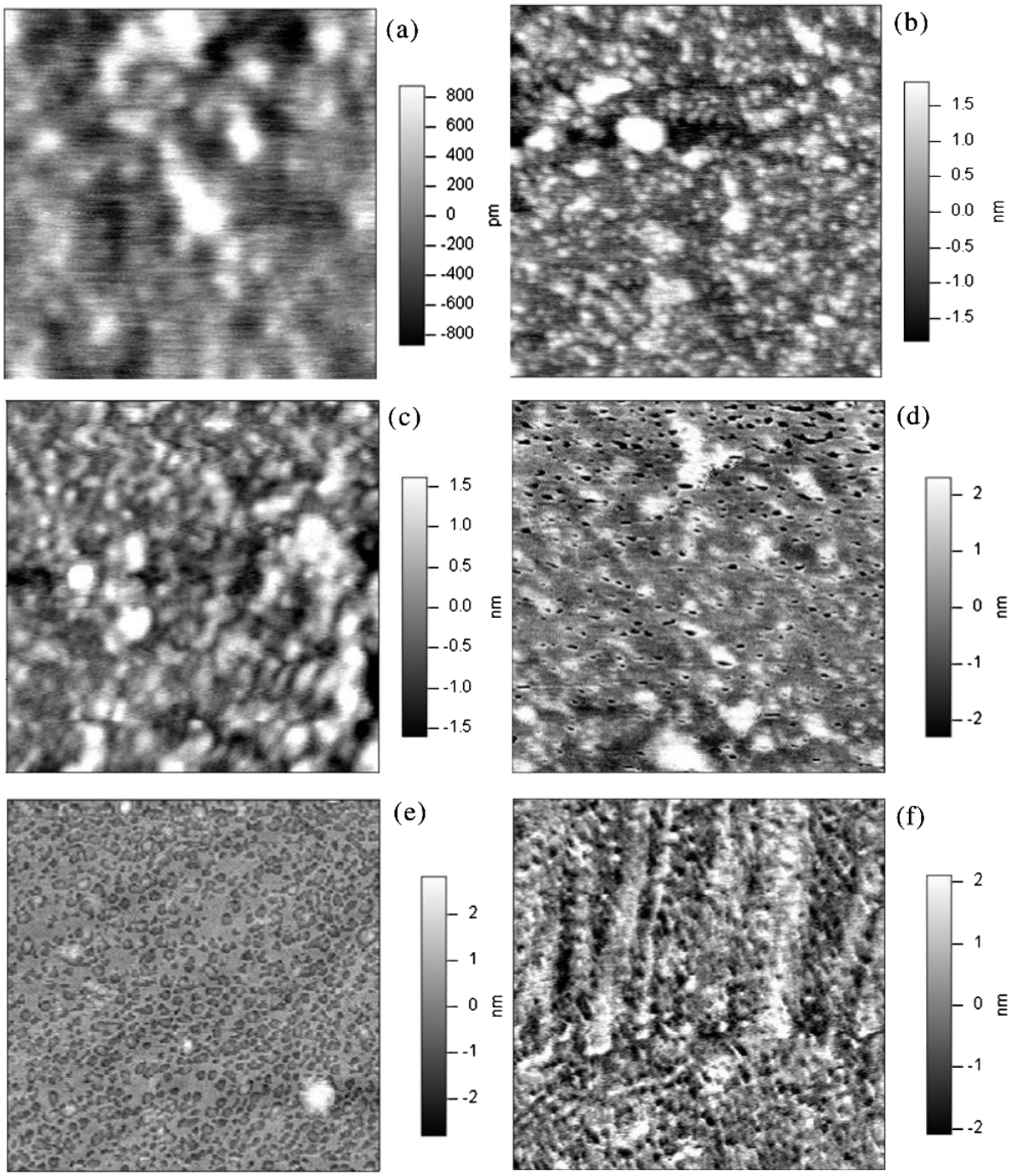

Figure 8. Six topography images (800 × 800 nm^2) of a GaN thin film scanned by (a) a commercial AFM cantilever tip, (b) our CNT probe made by UHV TEM in figure 7(a), and (c)–(f) the conventional CNT probe in figure 7(b). We can observe detailed characteristics in (b), where the resolution of <5 nm is confirmed by the various grain sizes. In (c) the AFM image displays a poorer resolution than (b), coming possibly from the excessively long CNT probe. In (d) the AFM image shows the concave artefact regarding the deformation of the CNT end. In (e) the AFM image shows the deckle edges along every grain boundary. The deckle edges result from the coupling of the flicking CNT probe. In (f) an AFM image having totally wrongly measured topography signals arises from the coexistence of the artefacts described in (d) and (e).

the protruding points. Comparing figures 8(b) and (d), the topography signals appear to be opposite to each another in the two AFM images; the grains in figure 8(b) are protruding, while those in figure 8(d) are concave. The cause of this phenomenon may be due to the deformation of the CNT tube end [31]. When the CNT probe scans over the grains in figure 8(b), the end of the exposed long CNT segment is deformed, resulting in a CNT probe length difference of several nanometres. Then, the tapping amplitude is increased beyond the setpoint. Hence, the piezotube will elongate to feedback the amplitude difference, leading to the holes in figure 8(c). This phenomenon is a typical artefact of the long flexible CNT (usually longer than 200 nm for the conventional ones), and it may worsen when we employ a SWCNT, which was originally

thought to render the highest resolution. The evidence of the deformation can be observed by comparing the two images in figure 7(b), which are in fact the two TEM images of the same CNT probe before (left side) and after (right side) the AFM scans, where a tiny bend at the CNT end appears in the right image. Our short CNT probe (<100 nm) is relatively less flexible and obviously eliminates this artefact as figure 8(b) shows. As for figure 8(e), we can observe many deckle edges along every grain boundary, which were discovered to come from the flicking CNT probe [32]. In detail, when the conventional CNT probe scans over a grain, the grain boundary will easily induce in a long CNT a flicking resonance which couples to the tapping frequency, resulting in another artefact of deckle edges. Again, our short and well welded CNT probe, which leads to a rigid structure, apparently displays no such an artefact. Figure 8(f) is a special case depicting the coexistence of the CNT deformation and flicking, where many concaves can be seen and the whole image looks perturbed by the coupling of the flicking and tapping resonances, leading to a totally incorrectly measured topography by amplitude-modulation feedback control. For the situations described in figures 8(d)–(f), the user-selected driving amplitude is also thought to be set too large, causing a strong interaction between tip and surface, which in turn results in a CNT deformation and flicking resonance. However, it is essential that the driving amplitude should be large enough to maintain a stable tapping cantilever upon the van der Waals interaction. Therefore, a shorter and more rigid CNT probe, such as the one shown in figure 7(a), is urgently needed for nanometre precision, which burgeoning nanoscience and nanotechnology now demand.

Two kinds of metal-coated commercial cantilevers are used to fabricate CNT probes in this paper. One is a PtIr/Cr coated n^+-Si cantilever, NANOSENSORS PointProbe EFM. The PtIr tip is for the conductive SPM measurement. CNT-probed electrostatic force microscopy (EFM) has enhanced its resolution to within 10 nm [24, 29]. We usually produce a CNT probe for EFM at a length of 300 nm because the bias at lift mode will burn off the CNT layer by layer. The other kind is a Au/Cr coated n-Si cantilever, MikroMasch NSC36 and CSC38, in which the NSC is for the tapping mode and the CSC for the contact mode. This kind of tip is for a typical AFM measurement. All the topography measurements in this paper were done using a commercial AFM system, Asylum Research MFP-3D, with a maximum scan area size of 90 × 90 μm^2 and a maximum piezotube elongation of 10 μm.

8. Conclusion

In summary, we have demonstrated a method for the fabrication of CNT probes using the UHV TEM system. The two 3D sub-nanometre movable holders and the *in situ* imaging inside the UHV chamber enable all the procedures to be done with a single SPM@TEM system. The *in situ* work allows us to select a CNT of any preferred size. The selected CNT can be regarded as a nano-finger to remove contaminants from the cantilever tip. Controlling the contact portion between the CNT and the tip makes the effective length of CNT probe user-defined. Thus, a short CNT probe less than 100 nm becomes possible. We further weld the CNT onto the tip surface via the TEM e-beam exposure under UHV conditions, at which contamination does not occur, as opposed to exposure in an SEM. More importantly, the apex of the CNT probe can be trimmed to less than 5 nm, so that the dimension is close to, but more rigid than the SWCNT, due to the MWCNT base.

The quality of our CNT probe is examined by the typical tapping-mode AFM measurement. For the measured topography on the GaN thin film, the lateral grain size is resolved to <5 nm. We have found that the height signal of the grains gives a perturbation between figures 8(c) and (f). The reason has been attributed to the excessive length, CNT deformation and flicking CNT. We believe our CNT probe, greatly improved over conventionally employed methods, will push the application of CNT-probed scanning probe microscopy to the next stage.

Acknowledgments

Yuan-Chih Chang would like to thank our previous colleagues in IPAS, Yang-Shan Huang and Yuan-Hong Liaw, for their contributions in the integration of the SPM@TEM system. Shu-Cheng Chin would like to thank Yu-Chieh Wen and Chi-Kuang Sun from NTU and Jen-Inn Chyi from NCU for providing the GaN sample, Wei-Bin Su in IPAS for his helpful discussion, and Chi-Ann Yih from UCLA for her kind help. This work is sponsored by the National Science and Technology Programme for Nanoscience and Nanotechnology managed by the National Science Council, under grant NSC97-2120-M-001-008.

References

[1] Binnig G, Quate C F and Gerber Ch 1986 *Phys. Rev. Lett.* **56** 930–3
[2] Magonov S N, Qvarnström K, Elings V and Cantow H J 1991 *Polym. Bull.* **25** 689–94
[3] Radmacher M, Tillamnn R W, Fritz W and Gaub H E 1992 *Science* **257** 1900–95
[4] Chang Y C, Lo Y H, Lee M H, Leng C H, Hu S M, Chang C S and Wang T F 2005 *Biochemistry* **44** 6052–8
[5] Binning G, Rohrer H, Gerber Ch and Weibel E 1982 *Phys. Rev. Lett.* **49** 57–61
[6] Zhong Q, Inniss D, Kjoller K and Elings V B 1993 *Surf. Sci.* **290** L688–92
[7] Iijima S 1991 *Nature* **354** 56–8
[8] Iijima S, Ichihashi T and Ando Y 1992 *Nature* **356** 776–8
[9] Dai H, Hafner J H, Rinzler A G, Colbert D T and Smalley R E 1996 *Nature* **384** 147–50
[10] Tong J and Sun Y 2007 *IEEE Trans. Nanotechnol.* **6** 519–23
[11] Hafner J H, Cheung C L and Lieber C M 1999 *Nature* **398** 761–2
[12] Nishijima H, Kamo S, Akita S, Nakayama Y, Hohmura K I, Yoshimura S H and Takeyasu K 1999 *Appl. Phys. Lett.* **74** 4061–3
[13] Martinez J, Yuzvinsky T D, Fennimore A M, Zettl A, García R and Bustamante C 2005 *Nanotechnology* **16** 2493–6
[14] Frank S, Poncharal P, Wang Z L and de Heer W A 1998 *Science* **28** 1744–6
[15] Akita S, Ohashi M and Nakayama Y 2005 *Japan. J. Appl. Phys.* **44** 1637–40

[16] Nanofactory Instruments Website: http://www.nanofactory.com
[17] Kondo Y and Takayanagi K 2000 *Science* **289** 606–8
[18] Chang Y C, Liaw Y H, Huang Y S, Hsu T, Chang C S and Tsong T T 2008 *Small* **4** 2195–8
[19] Ohnishi H, Kondo Y and Takayanagi K 1998 *Nature* **395** 780–3
[20] Binnig G and Rohrer H 1999 *Rev. Mod. Phys.* **71** S324–30
[21] Zhao M, Sharma V, Wei H, Birge R R, Stuart J A, Papadimitrakopoulos F and Huey B D 2008 *Nanotechnology* **19** 235704
[22] Chang Y C, Wang D C, Chang C S and Tsong T T 2003 *Appl. Phys. Lett.* **82** 3541–3
[23] Charrier D S H, Kemerink M, Smalbrugge B E, de Vries T and Janssen R A J 2008 *ACS Nano* **2** 622–6
[24] Tzeng S D, Wu C L, You Y C, Chen T T, Gwo S and Tokumoto H 2002 *Appl. Phys. Lett.* **81** 5042–4
[25] Hantschel T, Niedermann P, Trenkler T and Vandervorst W 2000 *Appl. Phys. Lett.* **76** 1603–5
[26] Xu Z W, Zhao Q L, Sun T, Guo L Q, Wang R and Dong S 2007 *J. Mater. Process. Technol.* **190** 397–401
[27] Cheung C L, Hafner J H, Odom T W, Kim K and Lieber C M 2000 *Appl. Phys. Lett.* **76** 3136–8
[28] Cheung C L, Hafner J H and Lieber C M 2000 *Proc. Natl Acad. Sci. USA* **97** 3809–13
[29] Chin S C, Chang Y C, Hsu C C, Lin W H, Wu C I, Chang C S, Tsong T T, Woon W Y, Lin L T and Tao H J 2008 *Nanotechnology* **19** 325703
[30] Chin S C, Chang Y C, Chang C S, Woon W Y, Lin L T and Tao H J 2008 *Appl. Phys. Lett.* **93** 253102
[31] Dietzel D, Marsaudon S, Aimé J P, Nguyen C V and Couturier G 2005 *Phys. Rev.* B **72** 035445
[32] Song W Y, Jung K Y, O B-H and Park B C 2005 *Rev. Sci. Instrum.* **76** 025107